Supplement of Clim. Past, 22, 1241–1254, 2026
https://doi.org/10.5194/cp-22-1241-2026-supplement

Supplement of

South Atlantic lipid biomarkers support synchronous Plio-Pleistocene global cooling: revising the ODP Site 1090 sea surface temperature record

Brianna Hoegler et al.

Correspondence to: Brianna Hoegler (brianna_hoegler@brown.edu)

SUPPLEMENTAL INFORMATION

Supporting Materials for Hoegler et al.

Methods: Determining Detection Limit

Tables S1 to S6

Figures S1 to S6

Supplemental References

Methods: Determining Detection Limit

To determine the limit of detection (LOD) for the C_{37} alkenones under the same analytical conditions used to construct the SST record, we conducted an experiment an extraction of marine sediment containing alkenones used as a laboratory reference analysed on the GC-FID with identical instrument settings (column, temperature program, and an injection volume of 10 µL out of a total sample extract of 210 µL) used during our ODP Site 1090 data collection. The standard was run at progressively lower concentrations, each 1/5 dilution of the previous, until the peak height of the C_{37} alkenones was approximately three times the baseline noise level, consistent with a signal-to-noise ratio of ~3 commonly used to define the LOD (Table S5). Based on this assessment and considering the sediment mass extracted for our samples (7–10 g per sample), we determined that the detection limit corresponds to approximately 0.6–1.0 ng C_{37} alkenones per gram of sediment (Table S6).

Table S1: Equations used as part of this study.

No.	Equation	Description	Citation
1	$U_{37}^{K\prime} = \frac{[C_{37:2}]}{[C_{37:2} + C_{37:3}]}$	Simplified alkenone unsaturation index	(Prahl et al., 1988)
2	$U_{37}^{K\prime} = 0.033(SST) + 0.044$	Linear, global core-top calibration of SST to $U^{K\prime}_{37}$	(Müller et al., 1998)
3	$U_{37}^{K} = \frac{[C_{37:2} - C_{37:4}]}{[C_{37:2} + C_{37:3} + C_{37:4}]}$	Alkenone unsaturation index	(Brassell et al., 1986)
4	$U_{37}^{K\prime} = 0.033(SST) + 0.043$	Linear, culture-based calibration of growth temperature to $U^{K\prime}_{37}$	(Prahl & Wakeham, 1987)
5	$inferred\ U_{37}^{K\prime} = \frac{U_{37}^{K} + (\%C_{37:4} \times 0.01)}{1 - (\%C_{37:4} \times 0.01)}$	Calculate inferred $U^{K\prime}_{37}$ from U^{K}_{37} and $\%C_{37:4}$	This study

Table S2: Composite Sections and Interval Shifts

Sample ID	Relevance to Composite Splice	Shipboard MCD	Shift Relative to shipboard MCD	New MCD
0—56.63 MCD Interval: Holes D and E				
177 1090D 1H 3A 27-29	Interval start	3.62	0	3.62
177 1090D 6H 4A 126-128	Interval end	56.63	0	56.63
56.64—61.59 MCD Interval: Hole E				
177 1090E 6H 2A 1-3	Interval start	56.64	0	56.64
177 1090E 6H 5A 46-48	Interval End	61.59	0	61.59
61.50—67.50 MCD Interval: Hole D				
177 1090D 7H 1A 46-48	Interval start	61.45	+0.05	61.50
177 1090D 7H 5A 46-48	Interval end	67.45	+0.05	67.50
67.50— MCD Interval: Hole E				
177 1090E 7H 1A 110-112	Interval start	66.20	+1.30	67.50
177 1090E 7H 4A 26-28	Interval end	69.86	+1.31	71.17

Table S3: Age model tie points (N=33)

MCD	Age (kya)	Implied Sedimentation Rate (cm/kyr)	Tie point notes
53.78	2500		Hodell et al., 2003
54.59	2580	1.012	
54.90	2602	1.409	MIS 104/G1 ~2614 ka
56.53	2717	1.417	~MIS G6
56.80	2740	1.174	
57.55	2808	1.103	MIS G10
57.80	2842	0.7353	MIS G12
58.27	2887	1.044	MIS G14
58.93	2935	1.375	MIS G16
59.20	2946	2.455	MIS G17
59.75	3017	0.7746	~MIS G20
60.25	3081	0.7812	MIS K1/K2
60.75	3154	0.6849	Top Mammoth between 1090E 6H 4A and 5A
61.70	3270	0.8190	
62.00	3295	1.200	MIS M2
62.29	3325	0.9667	MIS MG1; base Mammoth 1090D 7H 1A 125
62.68	3388	0.6190	MIS MG4/MG5
63.70	3533	0.7034	MIS MG9
64.54	3650	0.7099	MIS Gi3; top Gilbert between 1090D 7/2/145 and 7/3/5
64.775	3681	0.7581	~MIS Gi4/Gi5
65.075	3716	0.85714	~MIS Gi6/Gi7
65.40	3758	0.7738	
66.42	3831	1.397	MIS Gi12
67.05	3874	1.465	
67.85	3924	1.600	~MIS Gi16
68.435	3966	1.393	
69.05	4000	1.809	MIS Gi20
69.325	4019	1.447	
69.68	4040	1.690	MIS Gi22
70.22	4077	1.459	~MIS Gi23/Gi24
70.59	4116	0.9487	~MIS Gi25
71.04	4160	1.023	MIS Gi26
71.16	4176	0.7500	MIS Gi26/27

Table S4: %$C_{37:4}$ and SST (°C) of samples measured both on the GC-FID and HPLC

Sample ID	**Depth (MCD)**	**%$C_{37:4}$ (GC-FID)**	**%$C_{37:4}$ (HPLC)**	**$U^{K'}_{37}$ SST (°C, GC-FID)**	**$U^{K'}_{37}$ SST (°C, HPLC)**
ODP 177 1090 E 6W 2A 121-123	57.84	3.54	0	12.08	10.77
ODP 177 1090 E 6H 3A 11-13	58.24	4.69	0.24	16.92	13.43
ODP 177 1090 E 6H 3A 17-18	58.30	3.45	0.64	14.24	14.58
ODP 177 1090 E 6H 3A 31-33	58.44	2.55	0	14.81	13.91
ODP 177 1090 E 6H 3A 107-108.5	59.20	8.99	0	11.49	12.49
ODP 177 1090 E 6H 3A 111-113	59.24	6.87	0	12.28	13.92
ODP 177 1090 E 6 H 3A 131-133	59.44	7.56	0.55	13.94	13.36
ODP 177 1090 E 6 H 4A 1-3	59.64	4.99	0	14.81	14.50
ODP 177 1090 E 6 H 4A 16-18	59.79	6.39	0	15.52	15.10
ODP 177 1090 E 6 H 4A 106-108	60.69	3.39	0	16.05	15.08
ODP 177 1090 E 6 H 4A 111-113	60.74	6.51	0	10.93	10.52
ODP 177 1090 E 6 H 4A 121-123	60.84	3.57	0	14.39	14.29
ODP 177 1090 E 6 H 5A 6-8	61.19	2.04	0.12	12.84	12.81
ODP 177 1090 E 6 H 5A 96-98	61.95	4.20	3.78	14.40	13.96
ODP 177 1090 E 6 H 5A 101-103	62.00	6.57	0	12.93	11.86
ODP 177 1090 E 6 H 5A 146-148	62.45	3.04	1.21	14.85	14.34

Table S5: LOD raw data

Sample	Area C_{36}	Area C_{37}	Area $C_{37:3Me}$	Area $C_{37:2Me}$	Height C_{36}	Height C_{37}	Height $C_{37:3Me}$	Height $C_{37:2Me}$
LOD A	60.9122	60.4631	63.8035	115.6007	16.5584	15.6734	13.9604	25.1103
LOD B	54.3661	53.9451	10.9014	20.2913	14.8144	13.7195	2.3841	4.1504
LOD C	48.7764	48.3203	1.6641	3.1922	13.0966	12.7265	0.3979	0.7024
LOD D	49.6348	49.1021	0.4448	0.623	13.4931	12.6407	0.0986	0.1497
LOD E	43.818	43.4859	0.3213	0.7505	11.9728	11.3733	0.1107	0.1872
LOD F	41.425	41.1074	0.1142	0.5133	11.3357	10.7652	0.0672	0.1254

NOTE: The green highlight denotes the sample where the height of the $C_{37:2}$ and $C_{37:2}$ peaks were found to reach the detection limit of approximately 3x the height of the baseline noise, ~0.0550.

Table S6: LOD calculations

Parameter	Calculation	LOD A	LOD B	LOD C	LOD D	LOD E	LOD F
concentration $C_{37:3}$ (ppm)	2 ppm * ($C_{37:n}$ peak area) / (internal standard area)	1.78	0.348	0.0625	0.0156	0.0195	0.0125
concentration $C_{37:2}$ (ppm)		3.20	0.605	0.110	0.0237	0.0329	0.0233
mass injected $C_{37:3}$	concentration * volume injected (mL)	0.00178	0.000348	0.000625	0.000156	0.000195	0.000125
mass injected $C_{37:2}$		0.00320	0.000605	0.00110	0.000237	0.000329	0.000233
mass in sample $C_{37:3}$ (µg)	mass injected * (210 µL / injection volume)	0.374	0.0730	0.0131	0.00328	0.00409	0.00262
mass in sample $C_{37:2}$ (µg)		0.673	0.127	0.0232	0.00497	0.00691	0.00489
$C_{37:3}$ concentration in sediment (7g) (ng/g)	1000 ng/µg * mass in sample / sediment mass (7 g)	53.4	10.4	1.88	0.468	0.584	0.375
$C_{37:2}$ concentration in sediment (7g) (ng/g)		96.1	18.2	3.31	0.711	0.988	0.699
$C_{37:3}$ concentration in sediment (10g) (ng/g)	1000 ng/µg * mass in sample / sediment mass (10 g)	37.4	7.30	1.31	0.328	0.409	0.262
$C_{37:2}$ concentration in sediment (10g) (ng/g)		67.3	12.7	2.32	0.497	0.691	0.489

NOTE: The green highlight denotes the sample where the height of the $C_{37:2}$ and $C_{37:2}$ peaks were found to reach the detection limit of approximately 3x the height of the baseline noise, ~0.0550. 7g sediment represents the low end of the extracted mass range, while 10 g sediment represents the high end.

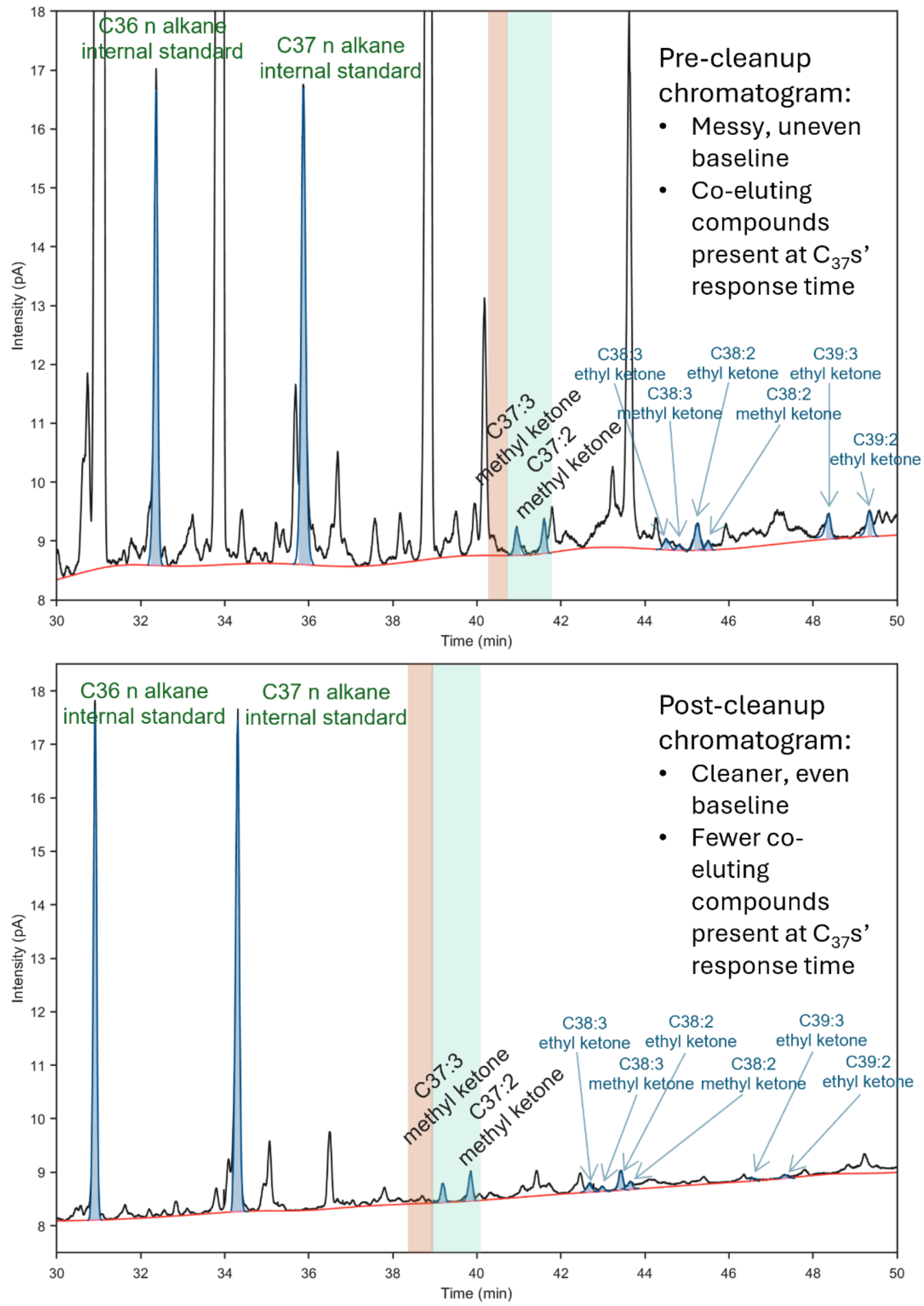

Fig. S1: Example chromatogram (sample: 1090D 7H 4A 124-126) showing pre- (above) and post-cleanup (below) GC-FID results. Our internal standards are labelled in green, and the C_{37} ketones are labelled in black; other ketones of interest are labelled in smaller, blue font. The green highlight shows where we expect to find $C_{37:2}$ and $C_{37:3}$ alkenone signals, and the orange highlight shows where a $C_{37:4}$ signal would elute. After cleanup, we observe a cleaner, less uneven baseline and fewer co-eluting compounds in the C_{37} alkenones' elution times.

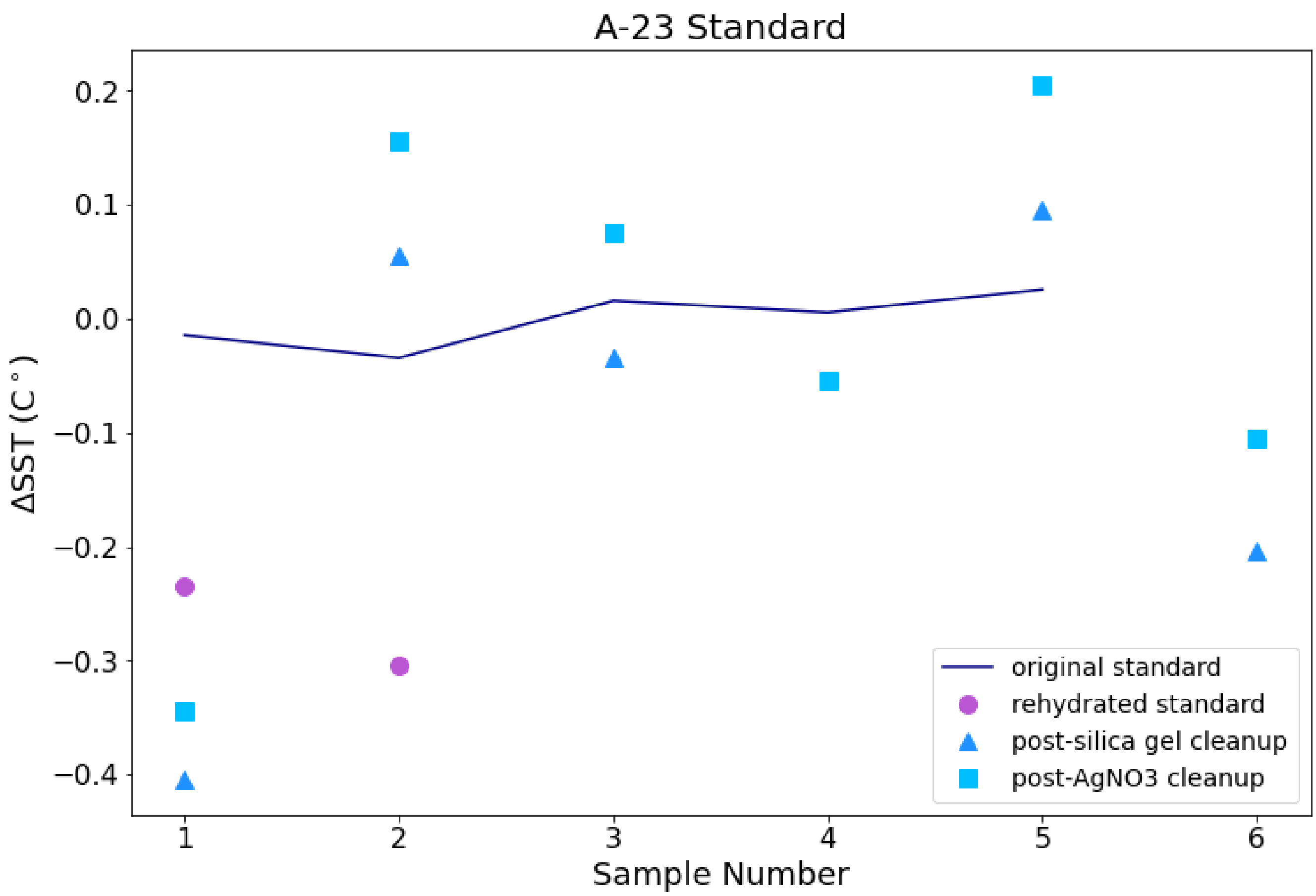

Fig. S2: The resulting difference in $U^{K'}_{37}$-based SST between the average SST derived from measurements of our unadulterated in-house alkenone standard (dark blue line) and that derived from the rehydrated in-house standard, in-house standard that was subjected to cleanup by just silica gel columns, and in-house standard that underwent cleanup with both silica gel and silver nitrate. All samples that underwent both forms of cleanup were well within our window of calibration error of 1.5°C.

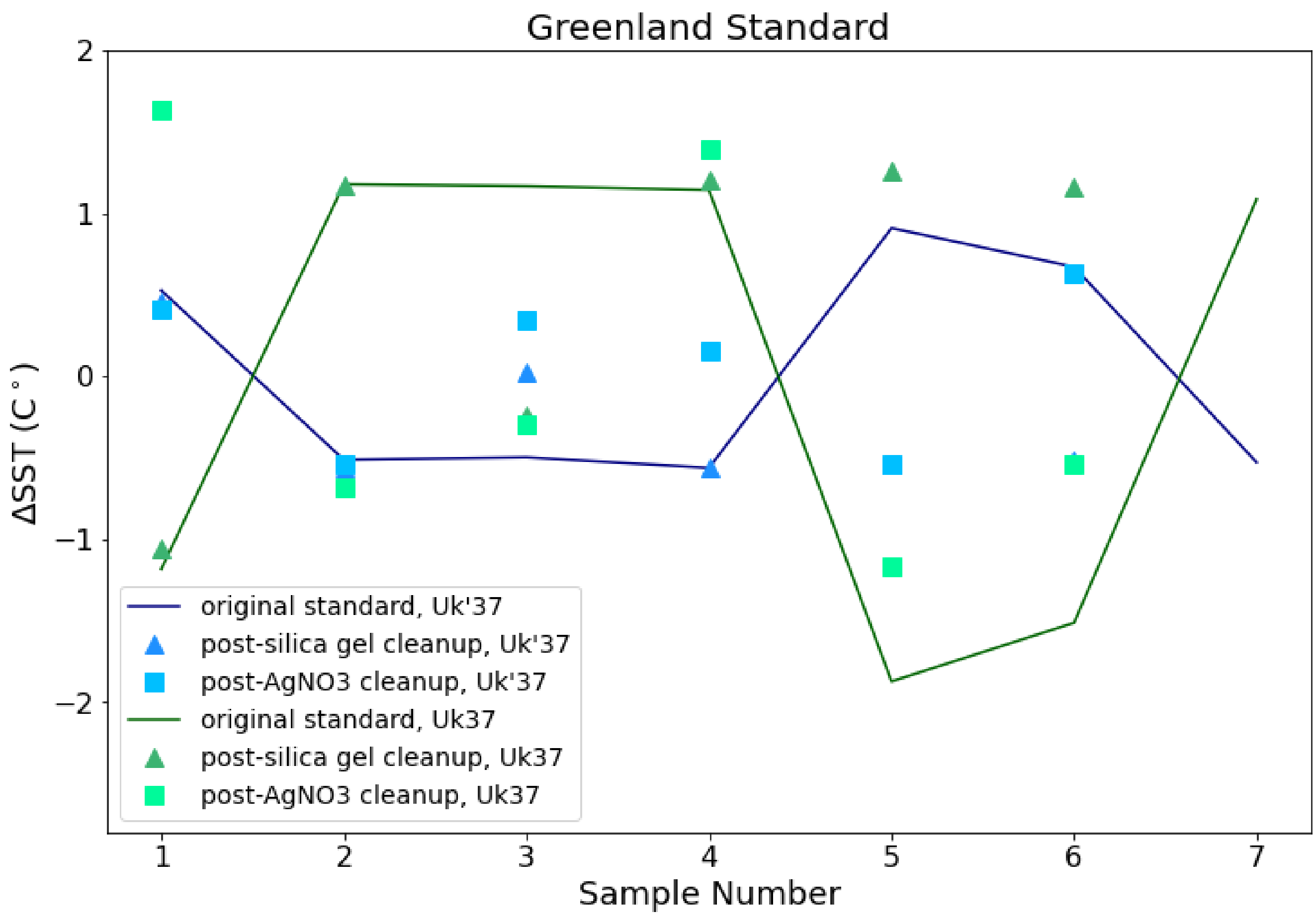

Fig S3: The resulting difference in $U^{K'}_{37}$-based (blue) and U^{K}_{37}-based (green) SST between the average SST derived from measurements of our unadulterated Greenland standard (dark blue/green lines) and those derived from the rehydrated Greenland standard, Greenland standard that was subjected to cleanup by just silica gel columns, and Greenland standard that underwent cleanup with both silica gel and silver nitrate. All SST estimates derived using samples that underwent both forms of cleanup and the $U^{K'}_{37}$ unsaturation index were within our window of calibration error of 1.5°C.

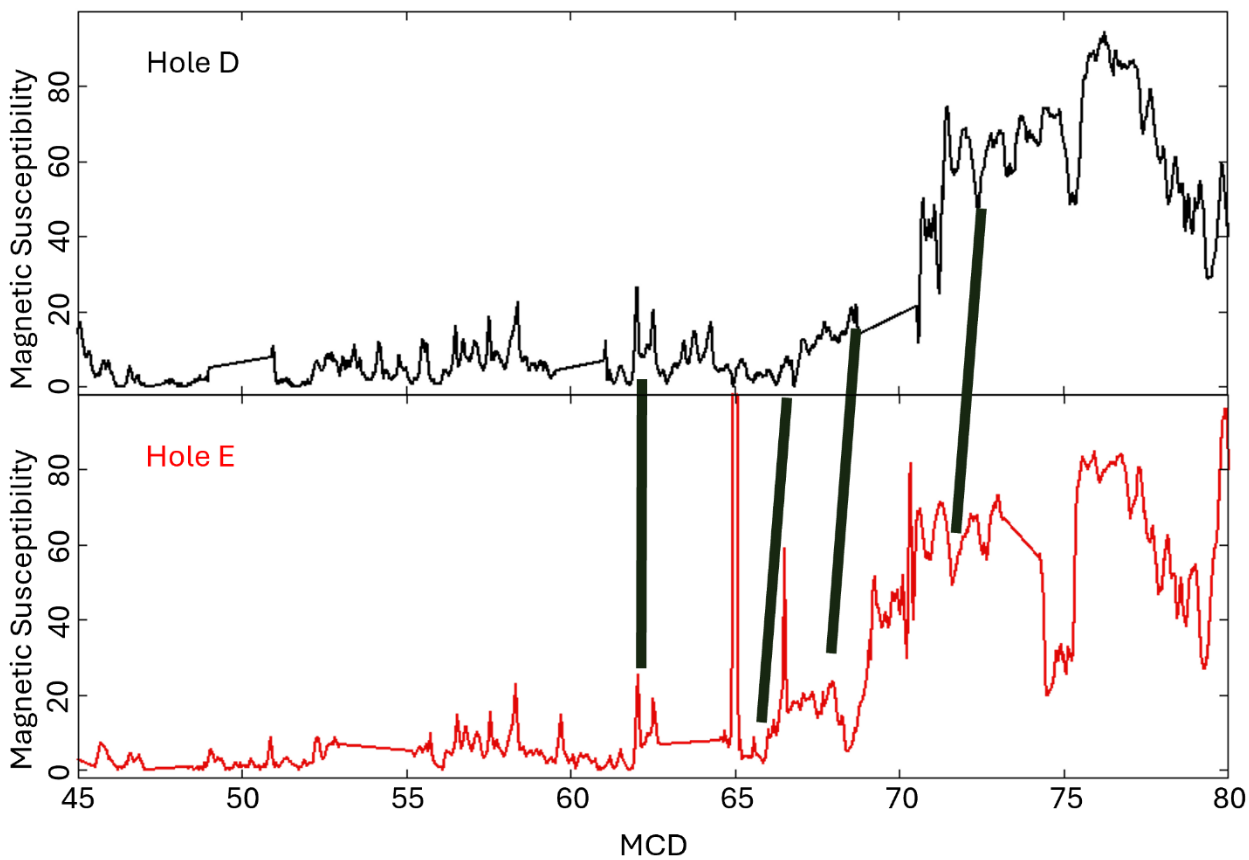

Fig S4: Magnetic susceptibility measurements from Holes D and E at ODP Site 1090 were utilized to construct our composite sediment record (Shipboard Scientific Party, 1999). Shipboard MCD is used here.

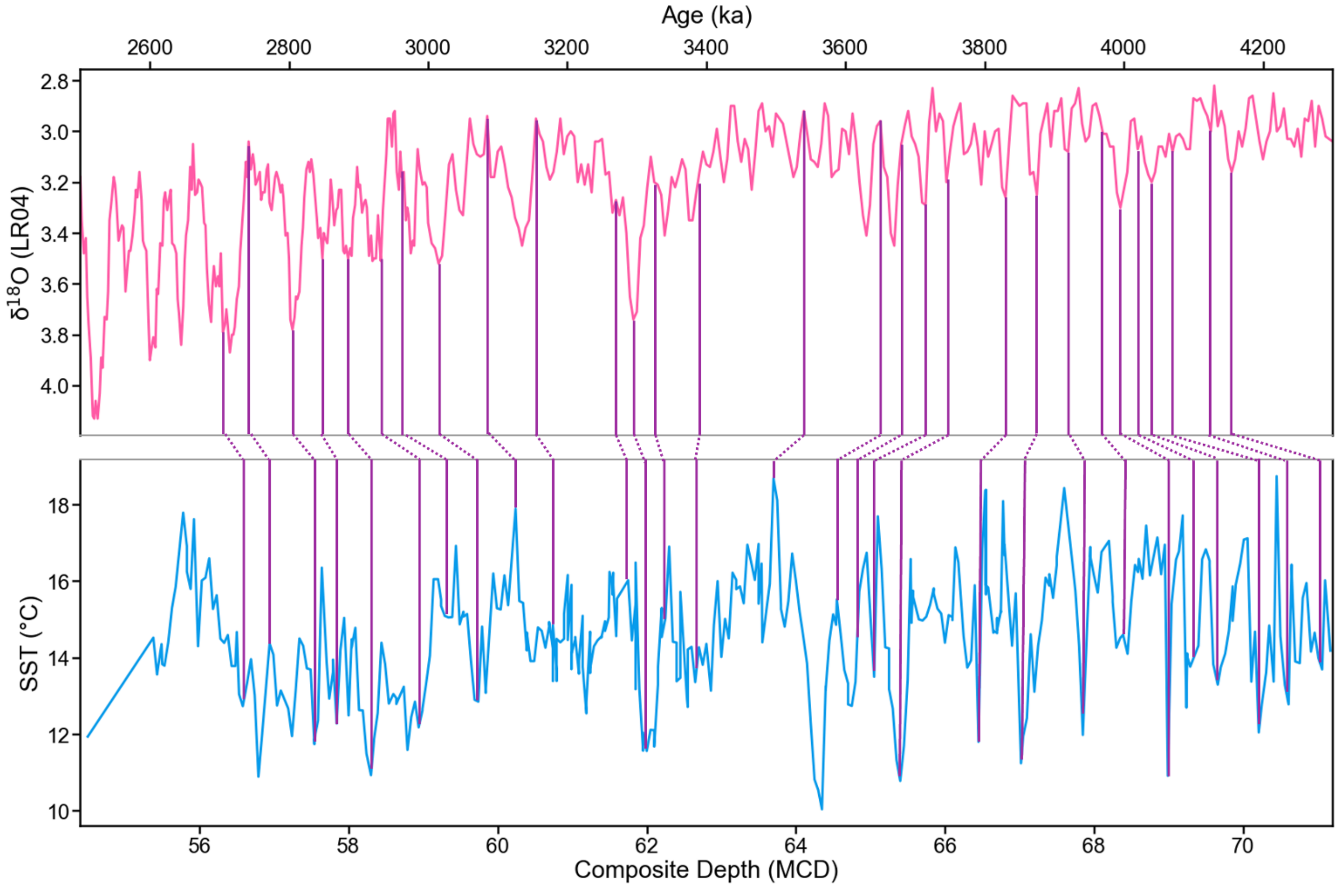

Fig. S5: Tie lines were established for our ODP Site 1090 age model by aligning our SST record with variations in the LR04 benthic oxygen isotope stack (Lisiecki & Raymo, 2005).

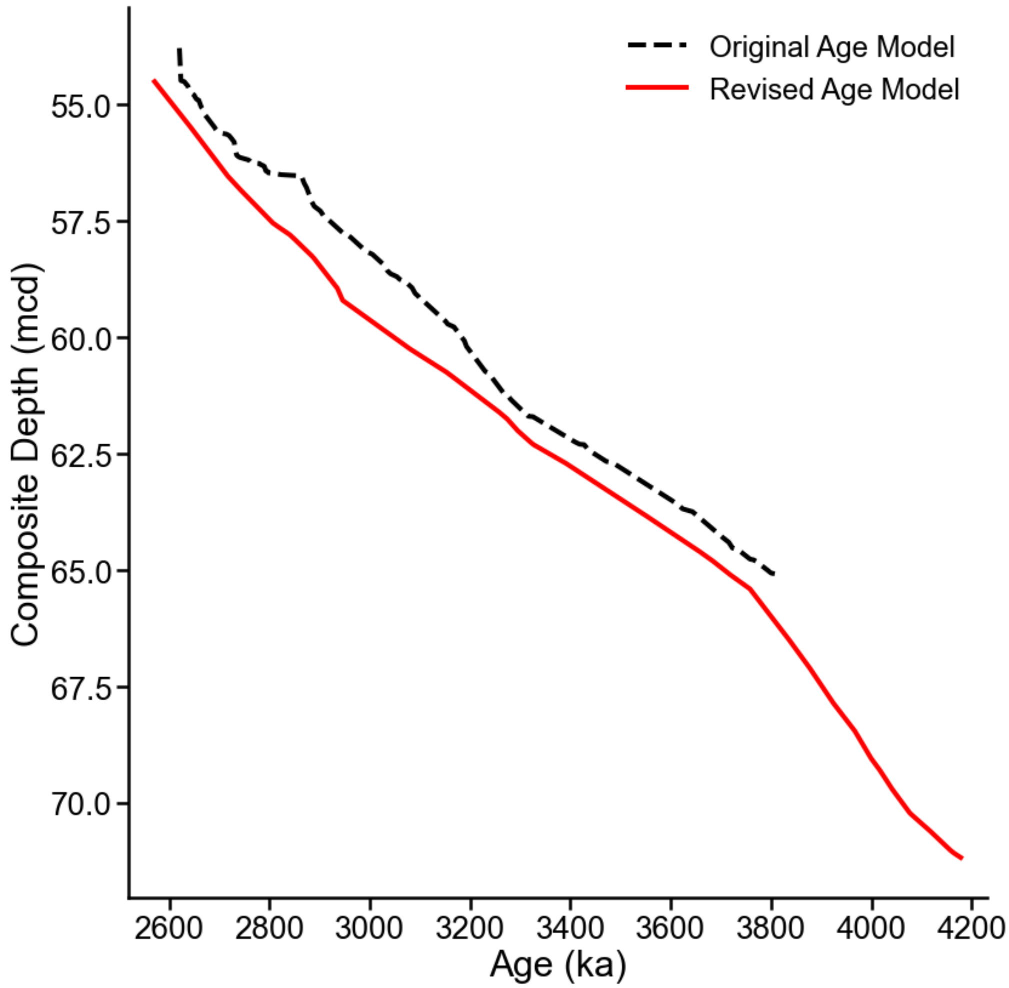

Fig. S6: Age-depth plots comparing Martínez-Garcia et al.'s (2011) original age-depth model (dashed black line) to the age-depth model produced as a part of this study (solid red line). Our age model avoids large changes in sedimentation rate (Table S3) while also extending the ODP Site 1090 alkenone-based SST record from ~3.8 Ma to ~4.18 Ma.

Supplemental References

Brassell, S. C., Eglinton, G., Marlowe, I. T., Pflaumann, U., and Sarnthein, M.: Molecular stratigraphy: A new tool for climatic assessment, Nature, 320, 129–133, https://doi.org/10.1038/320129a0, 1986.

Hodell, D. A., Charles, C. D., Curtis, J. H., Mortyn, P. G., Ninnemann, U. S., and Venz, K. A.: Data report: Oxygen isotope stratigraphy of ODP Leg 177 Sites 1088, 1089, 1090, 1093, and 1094, in: Proc. ODP, Sci. Results, Vol. 177, edited by Gersonde, R., Hodell, D. A., and Blum, P., 1–26, 2003, available at: http://www-odp.tamu.edu/publications/177_SR/VOLUME/CHAPTERS/SR177_09.PDF

Müller, P. J., Kirst, G., Ruhland, G., von Storch, I., and Rosell-Melé, A.: Calibration of the alkenone paleotemperature index $U_{37}K'$, Geochimica et Cosmochimica Acta, 62, 1757–1772, https://doi.org/10.1016/S0016-7037(98)00097-0, 1998.

Prahl, F. G., Muehlhausen, L. A., and Zahnle, D. L.: Further evaluation of long-chain alkenones as indicators of paleoceanographic conditions, Geochimica et Cosmochimica Acta, 52, 2303–2310, https://doi.org/10.1016/0016-7037(88)90132-9, 1988.

Prahl, F. G. and Wakeham, S. G.: Calibration of unsaturation patterns in long-chain ketone compositions, Nature, 330, 367–369, https://doi.org/10.1038/330367a0, 1987.